

# Interval based Fault Detection and Exclusion for GNSS

Hani Dbouk<sup>\*1</sup> and Steffen Schön<sup>2</sup>

<sup>1,2</sup>Institut für Erdmessung, Leibniz Universität Hannover,  
dbouk,schoen@ife.uni-hannover.de

**Keywords:** Intervals; Zonotope; Polytope; GNSS

## Introduction

Guaranteed protection levels of the Global Navigation Satellite System (GNSS) are of great importance, especially for the safety critical application such as: landing approach and navigation of autonomous vehicles. In order to guarantee the computed protection levels, reliable outlier detection and exclusion algorithms must be apply. In the past 30 years, different algorithms have been investigated based on statistical hypothesis testing. Thanks to their out-performance, the residual based test statistics and the solution separation have gained most interest compared to other algorithms. However, statistic-based fault detection and exclusion algorithms do not guarantee a safe navigation when the underlying assumptions on error probability density functions may not be fulfilled. In addition, interval-based fault detection techniques have been investigated in literature *e.g.*: q-relax intersection. This technique guarantees the protection level but it suffers from low accuracy in the multiple fault situation.

In this work, we propose a fault detection and exclusion technique based on deterministic observation intervals. The inconsistency of the positioning problem is indicated by the size of the polytope obtained from the intersection of the observation intervals. For the optimal case of no observation noise and no outliers, the polytope is a zonotope. Thus, we will use the normalized relative volume between a nominal polytope (zonotope) and the

actual non-regular polytope as indicator to derive an outlier detection.

The observation intervals are determined from sensitivity analysis of the correction models and the expert knowledge of the size of remaining errors. Applying the interval bounds on both direction of the observation transforms the navigation problem from a single point position to a solution set represented by non-regular polytope. If the observation intervals contain the actual observations, then the solution set guarantees to contain the true position. If biases occur for some observations, different situations can happen. For large biases, the solution set is empty which indicates the bias and can serve as detection criteria. When small biases occur, the solution set is not guaranteed and also not empty. In order to detect those type of biases, a threshold is proposed and applied on the relative volume which indicate the level of inconsistency between the intervals and the actual observations. Monte Carlo simulations are performed on different GNSS positioning scenarios for a better understanding of the inconsistency behavior.

## Methodology

The non-linear GNSS navigation equation Eq. (1), is linearized via Taylor expansion at an approximate initial position. As a result, we get the system of equations represented in Eq. (2). Then applying the interval bounds on the observed minus computed values, we get a system of inequalities Eq. (3) which can be interpreted as a hyperplan representation of a polytope.

---

<sup>\*</sup>Corresponding author.

$$l = \sqrt{(x_{sv} - x_u)^2 + (y_{sv} - y_u)^2 + (z_{sv} - z_u)^2} + c \cdot (dt_u - dt_{sv}) \quad (1)$$

$$\mathbf{A}d\hat{\mathbf{x}} = d\mathbf{l} \quad (2)$$

$$d\mathbf{l} - \Delta \leq \mathbf{A}d\hat{\mathbf{x}} \leq d\mathbf{l} + \Delta \quad (3)$$

where  $sv$  indicates the space vehicle and  $u$  the user,  $l$  is the pseudorange measurements,  $cdt_u$  and  $cdt_{sv}$  the receiver and satellite clock offset, respectively,  $\mathbf{A}$  the design matrix,  $d\hat{\mathbf{x}}$  the estimated state vector, and  $\Delta$  the interval error bound of the observations. Then a primal dual polytope algorithm is used to transform the hyperplane representation into a vertex representation of the polytope.

The shape, volume and position of the polytope depend on the observation errors, interval bounds, and satellites geometry. As the observation errors increase, the volume of the polytope decreases till it becomes empty for large outliers *i.e.*: the true observation is outside the interval bounds. To measure this inconsistency in the observations, the nominal polytope (zonotope) is computed and compared to the regular polytope, Eq. (4).

$$Inconsistency = V_r = \frac{V_Z - V_P}{V_Z} \quad (4)$$

## Results and Discussion

We perform a Monte Carlo simulation to understand the behavior of the inconsistency measures in terms of geometry,  $\Delta$  and biases. Fig. 1 shows the results of the simulation, where 7 different scenarios with different number of satellites in view and geometrical dilution of precision GDOP (Table 1) have been analyzed. 1000 epochs have been simulated for each run, where a ramp bias is introduced starting from epoch 100 and ending at epoch 500. We simulate GPS code measurements with white noise ( $0, \sigma = 1m$ ) and a clock error with linear drift and white noise ( $0, 1m$ ).

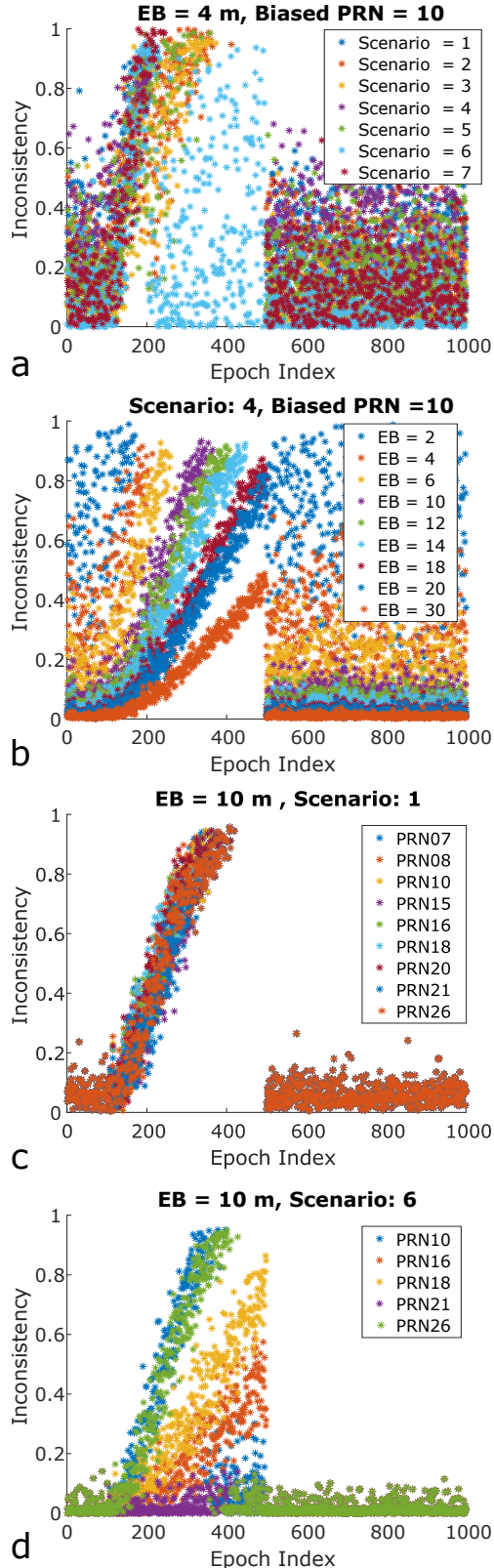


Figure 1: Inconsistency measures: a. different scenarios, b. different applied error bounds, c and d. different biased measurement.

Scen	1	2	3	4	5	6	7
$N_{SV}$	9	8	6	10	7	5	6
GDOP	2.3	2.4	3.3	2.0	3.3	11	9

Table 1: GDOP and number of satellites for each scenario in the Monte Carlo simulation.

Fig. 1.a shows the results when the  $\Delta$  are fixed to 4 meters and the biased satellite is the same for all scenarios. It is clear that different scenarios behave in a different way to the same biased satellite. In figure 1.b the scenario (4) and the biased satellite (PRN 10) is fixed while varying the error bounds  $\Delta$ . The inconsistency behaves in a different way with and without biases. As the error bound increases the mean value of the inconsistency decreases and the slope of the inconsistency in the biased region decreases and number of empty sets decreases.

Fig. 1.c and 1.d display the different biased satellites where the geometry and the  $\Delta$  were kept fixed. Fig. 1.c depicts a good geometry situation (scenario 1; GDOP = 2.3) and reveals the same effect for different biased satellites, while Fig. 1.d depicts the bad geometry (scenario 6; GDOP = 11) and implies different behavior of the inconsistency for different biased satellites. This behavior depends on the line-of-sight direction of the biased satellites and the geometry of the other satellites in view. A good explanation and demonstration is presented in [1].

The Monte Carlo simulation reveals the complexity of the inconsistency measures derived from the relative volume of polytopes. For simplicity and to test the algorithm on a real data, we apply a simple threshold test based on the mean value and the standard deviation of the relative volume. Fig. 2 shows the cumulative frequency of the 3D position error with and without applying the fault detection and exclusion on the inconsistency. The test shows a 25.6 % improvement in position where the root mean square of the po-

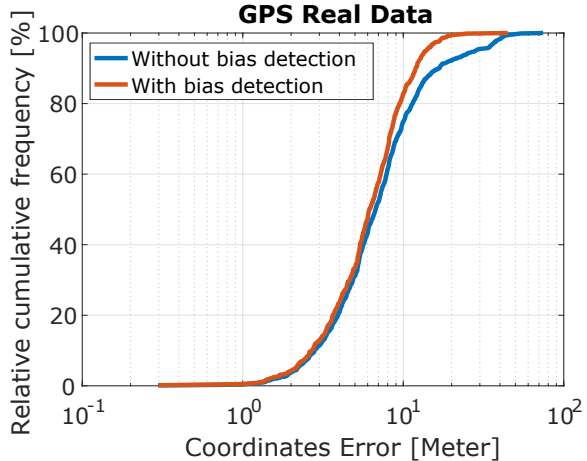


Figure 2: Cumulative frequency of the 3D coordinates error.

sition error decreases from 9 m to 6.7 m.

## Conclusions

In this study, a new fault detection and exclusion method is developed and tested with simulated and real data. First results show around 25 % improvement in the positioning error with simple threshold test. However, the behavior of the inconsistency measures is more complicated and varies from situation to another as the Monte Carlo simulation suggest. In the future more sophisticated test will be investigated.

## Acknowledgement

This work was supported by the German Research Foundation (DFG) as a part of the Research Training Group i.c.sens [GRK2159].

## References

- [1] H. Dbouk and S. Schön. Reliability and integrity measures of gps positioning via geometrical constraints. pages 730–743. Proceedings of the 2019 International Technical Meeting of The Institute of Navigation, Jan. 2019.